5. G. S. Pisarenko, V. A. Agarev, A. L. Kvitka, et al., Resistance of Materials [in Russian], Vyshcha Shkola, Kiev (1973).
6. V. I. Kosyak, Optimization of the Process of Failure of Round Rods in Bending in Connection with the Cutout of Rolled Stock, Author's abstract of PhD thesis, Kiev (1982).
7. E. N. Vysotskii, Investigation and Elaboration of the Process of Breaking Rolled Stock, Author's abstract of PhD thesis, Kramatorsk (1982).
8. V. V. Grishaev and E. N. Vysotskii, "Conditions of high-quality sorting of rolled stock by the method of breaking," in: All-Union Conference on the Elaboration and Industrial Implementation of New Methods of Machining and of Physicochemical Treatment (Moscow, December, 1988), Abstracts of Papers, Part 1, MVTU, Moscow (1988), pp. 50-51.
9. Yu. A. Kostandov and S. I. Fedorkin, "Propagation of fast cracks in hard polymers," Probl. Prochn., No. 9, 23-26 (1988).

MODELING OF THE EFFECTS OF ISOTROPIC STRENGTHENING IN NONPROPORTIONAL CYCLIC LOADING

M. V. Apaichev, I. A. Ivanov, and A. V. Pon'kin

UDC 539.374.001.57+620.178.3

On the basis of tests of the austenitic steel 03Kh21N32M3B with different programs of nonproportional loading including stages of various kinds of proportional cyclic loading and cyclic loading with constant strain intensity, the article analyzes the influence of the history of deformation on isotropic strengthening. It was established that in the material there exist several states of stabilization depending on the loading path, and to each of these states corresponds its own degree of isotropic strengthening. To express the experimentally observed effects, the article suggests determining equations in which isotropically kinematic strengthening is described on the basis of the evolution of a surface of "memory" in the space of plastic deformations. There is good agreement between the results of calculation and the experimental data.

1. To evaluate the serviceability of structures, their behavior in the dangerous (limit) state has to be calculated. In repeated variable loading with approximately 10^4-10^5 cycles during the period of operation, the onset of the dangerous state is characterized by inelastic deformations and low cycle fatigue associated with them. In this case it is an advantage in calculations of the reliability of structures to use mathematical models of inelastic cyclic deformation. These models are really based on experimental data on proportional cyclic loading but they are often used in calculations of structures whose deformation is substantially nonproportional. On the other hand, many data indicate that in proportional and nonproportional cyclic deformation materials have unequal rheological properties.

In the present work we investigated experimentally the effects which distinguish nonproportional cyclic deformation from proportional one, and we attempted to describe them on the basis of one of the alternatives of the theory of flow.

2. Tubular specimens (outer diameter 22 mm, wall thickness 2 mm) were tested in a special installation [1] under conditions of cyclic tension—compression with torsion. In the tests we specified the history of deformation. The line segments 1-4 (Fig. 1) are the paths of proportional loading with different orientation in the deviator plane $e_1 \sim e_2$:

$$e_1 = \frac{\sqrt{3}}{2}\left(\varepsilon - \frac{\sigma}{9K}\right); \qquad e_2 = \frac{\nu}{2},$$

where ε and ν are, respectively, the axial and shear strain in the specimen; σ is the axial stress; K is the bulk modulus of elasticity.

Chelyabinsk Polytechnic Institute, Chelyabinsk. Translated from Problemy Prochnosti, No. 7, pp. 47-51, July, 1991. Original article submitted November 29, 1990.

 0039-2316/91/2307-0770$12.50 © 1992 Plenum Publishing Corporation

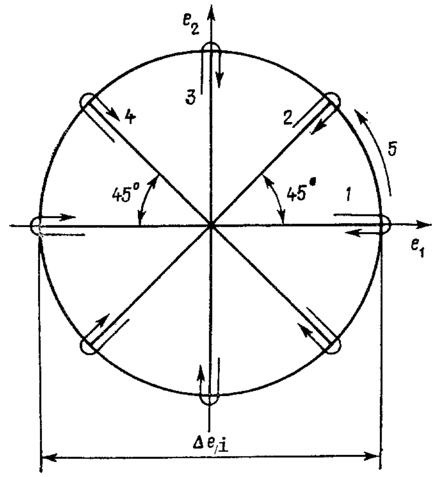

Fig. 1. Path of deformation in the deviator space.

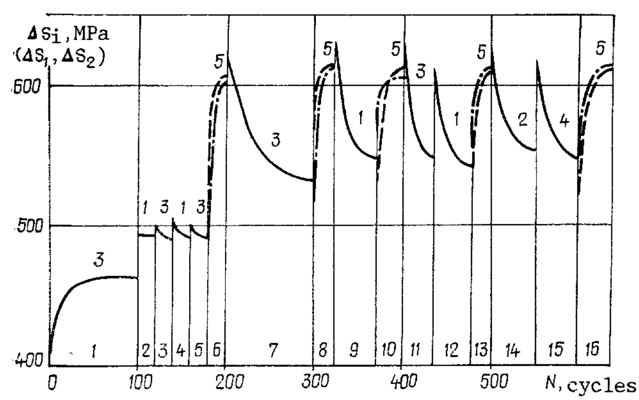

Fig. 2. Program and results of tests of a specimen with $\Delta e_i = 0.88\%$, $T = 20°C$.

The test program for each specimen consisted of several stages. At the stages of cyclic proportional deformation the specimen was loaded along one of the indicated paths up to stabilization of the properties of the material with subsequent "attenuation," viz., the same kind of cyclic deformation with the amplitude smoothly decreasing to zero. At the stage of nonproportional cyclic deformation loading was effected along a path with constant strain intensity (curve 5 in Fig. 1). At all the stages the maximal value of intensity of the double strain amplitude in a cycle $\Delta e_i = 2\sqrt{(e^2{}_1 + e^2{}_2)_{max}}$ was maintained equal.

Typical test results expressing the main effects of nonproportional loading are represented in Fig. 2. The axis of ordinates represents the double amplitude of strain intensity in a cycle $\Delta s_i = 2\sqrt{(s^2{}_1 + s^2{}_2)_{max}}$ ($s_1 = \sigma/\sqrt{3}$, $s_2 = \tau$, τ is the tangential stress), the axis of abscissas represents the number of load cycles. The numbers 1, 2, ..., 16 above the axis denote the number of the stage of loading, at each stage the form of the strain path is shown, the sections of "attenuation" are not shown in the figure.

Under the initial cyclic proportional deformation (stage 1) the material is strengthened with stabilization of the hysteresis loop after 40-60 load cycles. The stable diagram (according to test results of this and other specimens) does not depend on the orientation of the path in the deviator space, Il'yushin's postulate of isotropy [2] is fulfilled.

Subsequent loading along a path situated at an angle of 90° to the initial path (stage 2) showed that cyclic deformation in one direction brings about a strengthening of the material in other directions: the curve at stage 2 lies higher than the curve at stage 1. This is what the peculiar effect of "transverse" strengthening [3] consists in. Further alternation of stages of proportional deformation (stages 3, 4, 5) does not cause any noticeable changes in the strain diagrams which are close to stable.

Upon transition to nonproportional cyclic deformation with constant strain intensity (stage 6) the material is additionally strengthened, and after 10-15 load cycles it becomes stabilized. The dashed and dot-dash lines in Fig. 2, respectively, show the change of double stress amplitude in the cycle $\Delta s_1 = s_{1max} - s_{1min}$ and $\Delta s_2 = s_{2max} - s_{2min}$. Additional isotropic strengthening attains 35% of the value of Δs_i in the stable state of stage 1.

Subsequent proportional deformation (stage 7, torsion) leads to weakening of the material predominantly in the direction of deformation. This manifests itself in loading along path 5 at stage 8 where in the first cycles the material is more weakened in the direction of torsion than in the direction of tension—compression. Analogous effects are found at stages 9, 10.

Whereas after the stage of loading with constant strain intensity proportional deformation is successively effected along two mutually orthogonal paths in the deviator space (stages 11 and 12, 14 and 15), the change of double amplitude of the components s_1 and s_2 on the path 5 proves to be the same (stages 13 and 16).

3. To describe strengthening under nonproportional loading, Ohashi et al. [4] suggested a model of material (Ono's model) that takes the concept of the region of nonstrengthening deformations into account. The vector of the strain deviator $\mathbf{e}$ [2] is represented in the form of the sum of the elastic component $\mathbf{r}$ (correlated by Hooke's law with the stress) and the inelastic component $\mathbf{p}$:

$$\mathbf{e} = \mathbf{r} + \mathbf{p}, \quad \mathbf{r} = \mathbf{s}/2G. \tag{1}$$

In the stress space the loading surface

$$f = (\mathbf{s} - \mathbf{R})(\mathbf{s} - \mathbf{R}) - \left[k + \frac{L}{C_1}\rho\right]^2 \tag{2}$$

was introduced, where the additional stress $\mathbf{s}$ expresses kinematic strengthening; $\mathbf{R}$ is the vector of the stress deviator.

The associated law of plastic flow has the form

$$\dot{\mathbf{p}} = \begin{cases} \dfrac{(\mathbf{s} - \mathbf{R})\cdot\dot{s}}{(L + A)(\mathbf{s} - \mathbf{R})\cdot(\mathbf{s} - \mathbf{R})}(\mathbf{s} - \mathbf{R}) & \text{for } f = 0 \text{ and } \dot{\mathbf{s}}\cdot(\mathbf{s} - \mathbf{R}) > 0, \\ 0 & \text{for } f < 0 \text{ or } \dot{\mathbf{s}}\cdot(\mathbf{s} - \mathbf{R}) \leqslant 0, \end{cases} \tag{3}$$

where a dot denotes a scalar vector product; a dot above a symbol denotes differentiation with respect to time; L, A, C_1, k are constants of the material.

To describe isotropic strengthening (increase of the radius of the loading surface) in the space of inelastic deformations the region of nonstrengthening deformations was introduced:

$$g = (\mathbf{p} - \alpha)\cdot(\mathbf{p} - \alpha) - \rho^2 \leqslant 0, \tag{4}$$

which is bounded by a sphere henceforth called the memory surface (MS), with radius ρ and with the center determined by the vector α. The evolution of the memory surface is described by the following relations:

$$\left.\begin{aligned} \dot{\alpha} &= (1 - C_1)\dot{\mathbf{p}}\cdot\frac{\mathbf{p} - \alpha}{|\mathbf{p} - \alpha|}\cdot\frac{\mathbf{p} - \alpha}{|\mathbf{p} - \alpha|} \\ \dot{\rho} &= C_1\dot{\mathbf{p}}\cdot\frac{\mathbf{p} - \alpha}{|\mathbf{p} - \alpha|} \end{aligned}\right\} \text{for } g = 0 \text{ and } \dot{\mathbf{p}}\cdot(\mathbf{p} - \alpha) > 0, \tag{5}$$

$$\dot{\alpha} = 0, \ \dot{\rho} = 0 \text{ for } g < 0 \text{ or } \dot{\mathbf{p}}\cdot(\mathbf{p} - \alpha) \leqslant 0. \tag{6}$$

The law of change of the additional stress has the form

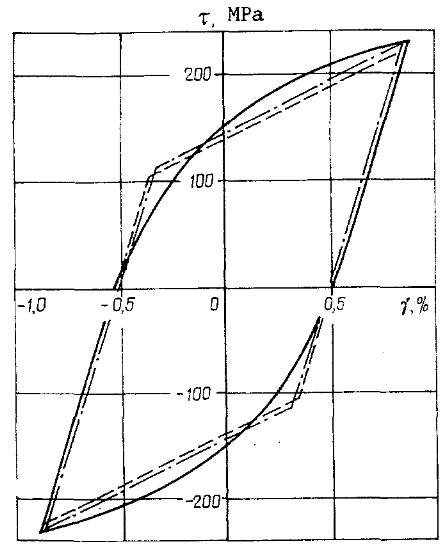

Fig. 3. Cyclic torsion (stable cycle) with Δe_i = 0.88%, T = 20°C. (Here and in Figs. 4, 5: solid line denotes experiment, dashed line the Ono model, dot-dash line the modernized alternative of the model.)

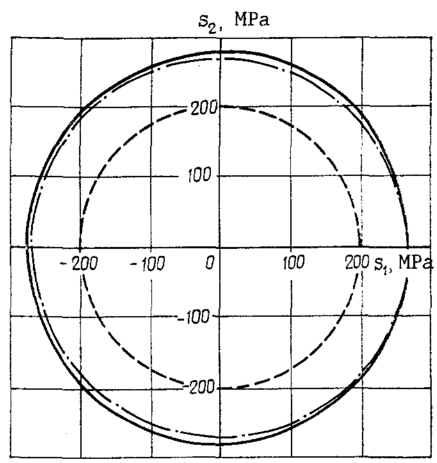

Fig. 4. Deformation along a path with constant strain intensity, with Δe_i = 0.88%, T = 20°C.

$$\dot{\mathbf{R}} = \begin{cases} \left[A + L\left(1 - \dfrac{\mathbf{p}-\alpha}{|\mathbf{p}-\alpha|} \cdot \dfrac{\dot{\mathbf{p}}}{|\dot{\mathbf{p}}|}\right)\right] \dot{\mathbf{p}} \text{ for } g = \\ = 0 \text{ and } \dot{\mathbf{p}} \cdot (\mathbf{p}-\alpha) > 0, \\ (A+L)\,\dot{\mathbf{p}} \text{ for } \quad g < 0 \quad \text{or} \quad \dot{\mathbf{p}} \cdot (\mathbf{p}-\alpha) \leqslant 0. \end{cases} \tag{7}$$

The radius of the yield surface (isotropic strengthening), like the memory surface, changes only when in the space of inelastic deformations the point corresponding to the current state lies on the memory surface and endeavors to move beyond its limits. This makes it possible to express additional isotropic strengthening upon transition from proportional to nonproportional loading. However, upon transition from nonproportional to proportional loading, weakening is not described by the model.

This shortcoming can be eliminated by introducing the following equations instead of (6):

$$\left.\begin{aligned} &\dot{\alpha} = 0 \\ &\dot{\rho} = -C_2 |\dot{\mathbf{p}}| \end{aligned}\right\} \text{ for } \quad g < 0 \quad \text{or} \quad \dot{\mathbf{p}} \cdot (\mathbf{p}-\alpha) \leqslant 0. \tag{8}$$

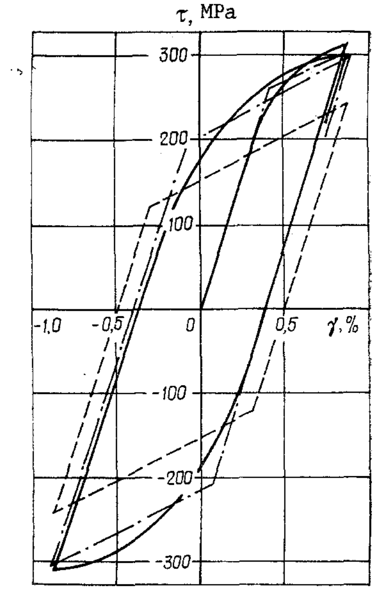

Fig. 5. Torsion after deformation along a path with constant strain intensity, with Δe_i = 0.88%, T = 20°C.

Dependences (8) together with (1)-(5), (7) make it possible to describe extension of the memory surface (and consequently isotropic strengthening) and in addition also a decrease of its dimensions (weakening).

Therefore in cyclic proportional loading the radius of the memory surface increases on some sections of the strain path (then the end of the vector **P** lies on the MS), on other sections it decreases (the imaging point is inside the MS). Stabilization is attained when there is dynamic equilibrium between the processes of strengthening and weakening. In case of deformation along a path with constant strain intensity, the point imaging the process of loading lies permanently on the memory surface. Stabilization is attained when the radius of the memory surface becomes equal to the amplitude of plastic deformation. Its value is much greater than the maximal radius of the MS under proportional loading with the same double amplitude of full strain intensity; thanks to that the model describes the effect of additional strengthening. Upon transition to proportional loading the radius of the memory surface begins to decrease, the material becomes weaker.

To identify the model we need data of cyclic tests obtained with loading along a path with constant strain intensity (from them the constants L, C_1 are determined) and with proportional loading (constants k, A, C_2). The first as well as the second kinds of tests can be carried out successively on one specimen.

4. The suggested alternative of the model was verified by comparing the results of calculation and of an experiment whose program included cyclic torsion to stabilization, damping, loading along a path with constant strain intensity, again damping, and cyclic torsion.

The parameters of the strain cycle are analogous to those described above.

The results of the calculations are presented in Figs. 3-5. In the calculations we used, as before [4], the bilinear approximation of the strain curves, and that is why the theoretical curves in Fig. 3 are broken. It can be seen in the figure that the elastoplastic hysteresis loop in torsion is described fairly accurately (within the limits of the chosen approximation) by both alternatives of the model. However, in the case of loading along a path with constant strain intensity (Fig. 4) the modernized alternative of the model describes the experiment better than Ono's model. The reason is that upon transition from proportional loading to nonproportional loading the memory surface in Ono's model increases solely in consequence of the misorientation of the stress and strain vectors (vectorial lag), and the result is that plastic deformation somewhat increases. This proves not to suffice for fully expressing the effect of additional strengthening. In the modernized model additional strengthening also occurs on account of the smaller radius of the MS (in comparison with Ono's model) in preliminary proportional loading.

In case of reversion to proportional loading (Fig. 5) the modernized model describes the experiment better since in distinction to Ono's model it gives expression to the process of weakening of the material.

LITERATURE CITED

1. M. V. Apaichev, D. A. Gokhfel'd, K. K. Dubovikov, and I. A. Ivanov, "Installation for studying the strain and strength characteristics of structural materials in nonproportional cyclic loading at normal and elevated temperatures," Probl. Prochn., No. 2, 117-117-120 (1985).
2. A. A. Il'yushin, Plasticity. Fundamentals of the General Mathematical Theory [in Russian], Izdatel'stvo Akademii Nauk SSSR, Moscow (1963).
3. A. Benallal and D. Marquis, "Constitutive equations for nonproportional cyclic elasto-viscoplasticity," Trans. ASME. J. Eng. Mater. Technol., 109, No. 4, 326-336 (1987).
4. Y. Ohashi, E. Tanaka, and M. Ooka, "Plastic deformation behavior of type 316 stainless steel subject to out-of-phase strain cycles," Trans. ASME. J. Eng. Mater. Technol., 107, No. 4, 286-292 (1985).

EFFECT OF STRUCTURAL PARAMETERS ON THE FATIGUE FAILURE OF CAST STEELS IN LOADING WITH LOW-CYCLE OVERLOADS

V. A. Tatarintsev and A. P. Shlyushenkov UDC 620.178.3:620.184.6:669.14.018

Experiments were carried out to examine the effect of structural parameters on the fatigue resistance in block loading with elastoplastic (low-cycle) overloads. Differences in the structural parameters were produced by heat treating 20GL steel by different techniques: normalizing, quenching and tempering, thermocyclic treatment (TCT), and by alloying. The results are presented of fractographic and metallographic analysis of specimens subjected to different heat treatments and fractured as a result of fatigue tests. An equation is derived for predicting the fatigue endurance of a specimen in block loading in relation to the mechanical characteristics and structural parameters of the steel.

For selection and comparative evaluation of materials in design of machine components, Shlyushenkov and Tatarintsev [1] proposed to use the results of fatigue tests in block (programmed) loading. For this purpose, the service regime of loading of the component is transformed to the block regime of variation of cyclic loading of the specimens which would ensure similar values of the fatigue damage of the material in the specimen in a testing unit and in a component under service loading. The parameters of the loading block are held constant for all specimen batches examined. The test results obtained in block loading are then used to construct distribution curves of the cyclic endurance of the specimens, and by comparing these curves it is possible to obtain information for the comparative evaluation of the efficiency of using a specific material and heat treatment, with an allowance made for the special features of the loading conditions.

Tests were carried out in regular and block cyclic loading on cylindrical specimens 8 mm in diameter with a circular groove 2 mm deep (stress concentration factor $\alpha_\sigma = 1.53$), made of normalized 20GL and 20 GFL steels and 20 GL steel subjected to different heat treatments. The mechanical characteristics of the steels and heat treatment conditions are presented in Table 1.

Tests of the specimens to failure were carried out in a MIP-8M fatigue testing machine with programmed loading with cantilever bending with rotation (a symmetric cycle of stress variation). To construct fatigue curves, 10-15 specimens were tested for each batch on different stress levels.

Bryansk Institute of Transport and Engineering. Translated from Problemy Prochnosti, No. 7, pp. 51-57, July, 1991. Original article submitted November 29, 1990.

0039-2316/91/2307-0775$12.50 © 1992 Plenum Publishing Corporation